Concanavalin A inhibits human liver cancer cell migration by regulating F-actin redistribution and assembly via MAPK signaling pathway

HAORAN JIANG, XIANXIN WEN, XUE ZHANG and BINGYU ZHANG

Chongqing Engineering Research Center of Medical Electronics and Information Technology, College of Bioinformatics, Chongqing University of Posts and Telecommunications, Chongqing 400065, P.R. China

Received February 23, 2022; Accepted September 14, 2022

DOI: 10.3892/ol.2022.13525

Abstract. Concanavalin A (Con A), the first and most typical representative of the legume lectin family, has a potent anti-liver cancer effect by inducing cell apoptosis and autophagy. However, its function in human liver cancer cell migration remains unclear. The present study investigated the effect of Con A on the viability and migration of human liver cancer cells with different metastatic abilities. It was found that Con A could reduce the viability of human liver cancer cells (HCCLM3, MHCC97L and HepG2) and human hepatocytes (MIHA). In addition, Con A could inhibit human liver cancer cell migration specifically without affecting hepatocytes. Sugar inhibition assay showed that glucose-related sugar binding sites played an important role in the inhibition of Con A on human liver cancer cell migration. In addition, Con A could affect HCCLM3 migration by activating ERK1/2, JNK1/2/3 and p38 signaling in the MAPK pathway. Moreover, Con A could regulate fibrous actin (F-actin) redistribution and assembly via the MAPK signaling pathway. However, Con A had no significant effect on the activation of matrix metalloproteinase (MMP)-2 and MMP-9 in HCCLM3 cells. In conclusion, Con A may bind to glucose-related receptor protein, activating ERK1/2, JNK1/2/3 and p38 signaling in the MAPK pathway, further contracting cells and reducing the content of F-actin of single cells to inhibit HCCLM3 cell migration. These results would deepen the links between human liver cancer cell migration and related glycoproteins or signaling molecules, and may provide a new perspective for Con A as a potential anticancer agent.

Correspondence to: Dr Bingyu Zhang, Chongqing Engineering Research Center of Medical Electronics and Information Technology, College of Bioinformatics, Chongqing University of Posts and Telecommunications, 2 Chongwen Road, Nanan, Chongqing 400065, P.R. China
E-mail: zhangbingyu@cqupt.edu.cn

Key words: cell migration, human liver cancer, concanavalin A, MAPK pathway, F-actin

Introduction

Tumors are the product of gene mutations. Their malignant capacity usually derives from abnormal function of mutant oncoproteins and aberrant signal transduction (1). Under abnormal molecular signal transmission, certain functional proteins would be modified by incorrect glycosylation under the action of the Golgi apparatus, and this abnormal glycosylation is closely associated with the malignant proliferation of tumor cells (2,3). Moreover, aberrant glycosylation of functionally membrane glycoproteins would affect adhesion or motility of tumor cells, resulting in invasion and metastasis. For example, high expression of sialoglycoconjugates in colorectal cancer is significantly associated with poor prognosis and lymph node metastasis (4). Altered sialylation of cancer cells was found to be closely associated with the malignant properties of invasiveness and metastasis (5).

Plant lectin is a kind of protein molecule derived from natural plants, which has been described as a class of toxic protein that exerts biological effects by binding specifically to glycan (6). As a toxic protein, plant lectin has been found to have anti-proliferative activity against tumor cells (7,8). In addition, based on the specific sugar-binding ability, plant lectin has also been applied to diagnose malignant and benign tumors with different degrees of glycosylation (9,10).

Liver cancer is the most frequent fatal malignancy. Previous studies showed that Concanavalin A (Con A), a plant lectin from Jack bean seeds, has a potent anti-liver cancer effect (11,12). Con A, after binding to the mannose moiety on the cell membrane glycoprotein, is internalized preferentially to the mitochondria, and then autophagy is triggered, which can lead to cell death (13). Moreover, Con A, as a T cell mitogen, can activate the immune response in the liver, which results in the eradication of the tumor in a murine *in situ* hepatoma model (14). However, there are limited studies on the effect of Con A on liver cancer cell migration, particularly the molecular mechanism based on the sugar-binding ability of Con A.

The current study explored the effect of Con A on the viability and migration of three human liver cancer cell lines with different metastatic ability, and further analyzed the possible sugar sites and related molecular mechanisms of the interaction between Con A and human liver cancer cells.

Materials and methods

Cell culture and Con A solution. The human liver cancer cell lines HCCLM3 (cat. no. C6303), MHCC97L (cat. no. C6586) and HepG2 (cat. no. C6346) were obtained from Beyotime Institute of Biotechnology, while the normal hepatocyte cell line MIHA was obtained from American Type Culture Collection (ATCC; cat. no. AC340123). Human liver cancer cells and hepatocytes were cultured in 25-cm^2 gas-permeable cell culture flasks (Wuhan HealthCare Biotechnology Co., Ltd.) in a cell incubator with an atmosphere of 5% CO_2 at 37˚C. Culture medium was changed every 3 days. High-glucose DMEM (Gibco; Thermo Fisher Scientific, Inc.) and standard RPMI-1640 medium (Gibco; Thermo Fisher Scientific, Inc.) were used for cell culture, and were supplemented with 10% fetal bovine serum (HyClone; Cytiva), 100 U/ml streptomycin and 100 U/ml penicillin (Biosharp Life Sciences). All cell lines were authenticated periodically by cell morphology monitoring and growth curve analysis, according to the ATCC cell line verification test recommendations.

The Con A powder used in the current study was purchased from Shanghai Aladdin Biochemical Technology Co., Ltd. Con A powder (10 mg) was dissolved in 1 ml PBS to prepare a stock solution of a concentration of 10 μg/μl, which was then diluted into several 2-μg/μl working solutions with PBS at a ratio of 1:4, and stored at -20˚C until use in subsequent experiments.

Cell viability assay. Cell Counting Kit (CCK)-8 assay was used to detect cell viability. First, cells were inoculated into 96-well plates at a density of $5x10^3$ cells/well. After the cell adhered and returned to their normal shape, they were serum-starved overnight and then treated with different concentrations of Con A (0, 1, 3, 5 and 10 μg/ml) for 12, 24 or 48 h. Following the indicated treatment time, 5 mg/ml CCK-8 reagent (0.5 mg/ml; Sigma-Aldrich; Merck KGaA) was added to each well and incubated with cells for 2 h at 37˚C. Lastly, the absorbance of the cells at a wavelength of 450 nm was measured with a spectrophotometer (Molecular Devices, LLC) to quantify the cell viability.

Cell migration assay. Transwell assay was used to detect cell migration. The experiment was performed in a 24-well plate, and the Transwell chamber (pore diameter, 8 μm; MilliporeSigma) was placed above the plate. After the cells were starved overnight in a cell culture flask, the cell suspension was prepared by adding serum-free medium, and subsequently inoculated into the upper layer of the chamber at a density of $5x10^4$ cells/100 μl. Next, 600 μl complete medium was added to the bottom of the plate to induce cell migration, and different concentrations of Con A (0, 1, 3, 5 and 10 μg/ml) were then added to the upper layer of the chamber containing the cell suspension for the cell migration assay. After 6 h, the chamber was removed from the well plate. The remaining upper cell suspension was adsorbed with a piece of cotton, and the cells in the upper chamber that failed to migrate were wiped slightly. Lastly, the cells that migrated to the lower layer of the chamber were fixed with 4% paraformaldehyde (Biosharp Life Sciences) for 10 min at room temperature, stained with 0.1% crystal violet (Shanghai Beyotime Biotechnology Co., Ltd.) for 30 min at room temperature and images were captured with an inverted light microscope (Olympus Corporation).

Sugar inhibition assay. D-glucose and D-mannose (Shanghai Aladdin Biochemical Technology Co., Ltd.) were used to detect the sugar-binding site between Con A and human liver cancer cells. A Con A + DMEM control group to verify whether D-glucose in high-glucose DMEM had an effect on the glucose binding ability of Con A. A total of 20 mg powdered glucose or mannose were dissolved in 10 ml sterile deionized water to generate working solutions with a concentration of 2 μg/μl, which were aliquoted and stored at -80˚C. Prior to cell viability and migration assays, high-glucose DMEM or the aforementioned sugar solutions were pre-incubated with Con A at a ratio of 1:1 at room temperature for 30 min, and cell viability or migration assays was then carried out.

Western blot analysis. Western blotting was used to detect protein expression of mitogen-activated protein kinases (MAPK) pathways in HCCLM3 cells. First, $5x10^4$ cells were inoculated on six-well plates. When the cell density reached ~70%, the cells were starved overnight and then treated with Con A (10 μg/ml) for 0, 15, 30, 60 or 120 min. After Con A treatment, total protein was extracted using cell lysis buffer (Shanghai Beyotime Biotechnology Co., Ltd.). The protein concentration was determined by the Lowry's method using bovine serum albumin (BSA; Shanghai Beyotime Biotechnology Co., Ltd.) as standard. Then, 50 μg total protein was loaded per lane. Upon electrophoretic separation by 12% SDS-PAGE, the proteins were electrotransferred onto 0.22-μm-pore Polyvinylidene fluoride (PVDF) membranes (MilliporeSigma). Next, TBS containing 0.1% Tween-20 (TBST) and 5% BSA were used to block the PVDF membranes at room temperature for 1 h. To analyze the effect of Con A on individual phosphorylated proteins in the MAPK pathway, the following antibodies were incubated with the membranes at 4˚C overnight according to the corresponding manufacturer's protocol: Anti-ERK1 [phosphorylated (p) T202/pY204] + ERK2 (pT185/pY187) rabbit monoclonal antibody [(mAb); 1:10,000, cat. no. ab76299; Abcam], anti-ERK1 + ERK2 rabbit mAb (1:10,000; cat. no. ab184699; Abcam), anti-JNK1 + JNK2 + JNK3 (pT183 + T183 + T221) rabbit mAb (1:10,000; cat. no. ab124956; Abcam), anti-JNK1 + JNK2 + JNK3 rabbit mAb (1:10,000; cat. no. ab179431; Abcam), anti-p38α/MAPK14 (pY322) rabbit polyclonal antibody [(pAb); 1:1,000; cat. no. 4511T; Cell Signaling Technology, Inc.], anti-p38α/MAPK14 rabbit mAb (1:1,000; cat. no. ab182453; Abcam) and anti-GAPDH rabbit mAb (1:10,000; cat. no. AP0063, Bioworld Technology, Inc.). Subsequently, the membranes were incubated with an HRP-conjugated antibody (1:10,000; cat. no. 511203; Zen-Bio) for 1 h at room temperature. Upon washing with TBST, the bands were visualized with an enhanced chemiluminescence kit (Thermo Fisher Scientific, Inc.) using a ChemiDoc Gel Imaging System (Clinx Science Instruments Co., Ltd.). ImageJ software (version 1.53e; National Institutes of Health) was used to analyze the optical density of the bands. GAPDH was used as a loading control for normalization.

Protein signaling inhibition assay. The ERK1/2 inhibitor U0126 (Dalian Meilun Biology Technology Co., Ltd.), the JNK1/2/3 inhibitor SP600125 (Shanghai Beyotime Biotechnology Co., Ltd.) and the p38 inhibitor SB203580 (Dalian Meilun Biology Technology Co., Ltd.) were used in the present study. The concentration of these three inhibitors was set to 5, 10 or 20 μM in order to determine the optimal effective concentration of inhibitors on HCCLM3 cells. Next, cells were pre-treated with U0126, SP600125 or/and SB203580 for 60 min at 37˚C before the addition of Con A (10 μg/ml) in the cell viability, cell migration or western blot assays.

Detection of fibrous actin (F-actin) filaments and cell spreading area. Immunofluorescence staining was used to detect the effect of Con A on the F-actin of cells. Cells were inoculated on 24-well plates, and when the cell density reached ~50%, the cells were starved overnight, and then treated with Con A (10 μg/ml) for 60 min. To block ERK1/2, JNK1/2/3 or/and p38 signaling, the cells were incubated with U0126, SP600125 or/and SB203580 for 60 min at 37˚C before Con A treatment. Subsequently, the cells were fixed with 4% formaldehyde for 30 min, treated with a permeabilization solution (0.25% Triton X-100; Beijing Solarbio Science & Technology Co., Ltd.) for 10 min and blocked with blocking solution (5% BSA; Beijing Solarbio Science & Technology Co., Ltd.) for 60 min at room temperature. Next, FITC phalloidin (Shanghai Beyotime Biotechnology Co., Ltd.) was added to stain F-actin in HCCLM3 cells overnight at 4˚C in the dark. Subsequently, the nuclei were labeled with 2 μg/ml DAPI (Shanghai Beyotime Biotechnology Co., Ltd.) for 10 min at room temperature. Lastly, images of the cells were captured using an inverted fluorescence trichromatic microscope (Olympus Corporation). The F-actin fluorescence intensity and spreading area of individual cells were semi-quantitatively evaluated by ImageJ software (version 1.53e; National Institutes of Health).

Gelatin zymography. Gelatin zymogram was used to detect the effect of Con A on the activities of matrix metalloproteinase-2 (MMP-2) and matrix metalloproteinase-9 (MMP-9). The HCCLM3 cells were inoculated on six-well plates. When the cell density reached ~90%, the cells were serum-starved overnight and then treated with Con A (10 μg/ml) for 6 h. Next, the supernatants were collected and centrifuged at 4,000 x g for 5 min at 4˚C. A BCA protein quantification kit (Nanjing KeyGen Biotech Co., Ltd.) was used to measure the protein concentration, and equal protein quantities (50 μg) were loaded per lane in the gel. A pre-stained protein molecular weight marker (Thermo Fisher Scientific, Inc.) was used as a size standard for protein electrophoresis. Gelatinase was concentrated and separated by 10% SDS-PAGE containing pigskin gelatin (Shanghai Beyotime Biotechnology Co., Ltd.). The separated gelatin containing MMP-2 and MMP-9 was then collected, eluted using 2.5% Triton-X-100 solution for 60 min and incubated in developing buffer (Tris 0.5 M, Brij35 0.2%, NaCl 2 M and $CaCl_2$ 50 mM, pH 7.6) for 16 h at 37˚C. Next, gelatin was stained by Coomassie Brilliant Blue (Beijing Solarbio Science & Technology Co., Ltd.) for 30 min at room temperature. Lastly, images of the gelatin were captured with a ChemiDoc Imaging System (Clinx Science Instruments Co., Ltd.). ImageJ software (version 1.53e; National Institutes of Health) was used to analyze the optical density of the bands.

Statistical analysis. SPSS software (version 21.0; IBM Corp.) was used for statistical analysis. Data are presented as the mean ± SD of ≥3 independent experiments, and were analyzed using one-way ANOVA followed by Bonferroni post hoc test for the comparison of multiple groups. $P<0.05$ was considered to indicate a statistically significant difference.

Results

Con A reduces the viability of human liver cancer cells and hepatocytes. CCK-8 assay was used to assess cell viability. As shown in Fig. 1, Con A inhibited the viability of three types of human liver cancer cells (HCCLM3, MHCC97L and HepG2) as well as hepatocytes (MIHA) in a time and concentration-dependent manner. When the concentration of Con A reached 10 μg/ml and was incubated with the cells for 48 h, the viability of the aforementioned four cell lines was inhibited to ~20% ($P<0.05$).

Con A inhibits the migration of three human liver cancer cell types, but had no effect on normal hepatocytes. Transwell assay was used to evaluate the effect of Con A on the migration of human liver cancer cells and normal hepatocytes. As revealed in Fig. 2A-D, Con A significantly inhibited human liver cancer cell migration ($P<0.05$) in a concentration-dependent manner. When the concentration of Con A reached 10 μg/ml and was incubated with the cells for 6 h, the migration of human liver cancer cells was almost completely inhibited. However, different concentrations of Con A (0, 1, 3, 5 and 10 μg/ml) had no significant effect on hepatocyte migration (Fig. 2E).

Con A inhibits human liver cancer cell migration through glucose-related sugar binding sites. To determine the glyco-binding site between Con A and liver cancer cells, exogenous glucose and mannose were incubated with Con A prior to cell migration assay. Since DMEM also contained glucose, a co-incubation experiment of DMEM with Con A was also performed. As shown in Fig. 3A-D, the addition of glucose (10 μg/ml) or mannose (10 μg/ml) alone had no significant effect on human liver cancer cell migration, but when Con A (10 μg/ml) was first incubated with glucose or mannose for 30 min, the migration level of human liver cancer cells in the Con A + glucose group was slightly restored ($P<0.05$), while the migration level of human liver cancer cells in the Con A + mannose group was the same as that of the Con A group.

In addition, compared with the almost complete inhibition of HCCLM3 cell migration in the migration assay (Fig. 2B), Con A (10 μg/ml) could only inhibit the viability of HCCLM3 cells to ~50% within 6 h (Fig. 3E). Fig. 3E also showed that co-incubation of Con A (10 μg/ml) with glucose (10 μg/ml) or mannose (10 μg/ml) did not restore the HCCLM3 cell viability reduced by Con A. As revealed in Fig. 3F-H, when Con A (10 μg/ml) was first co-incubated with DMEM, the effect of Con A on HCCLM3 viability and migration was not different from that of the Con A direct treatment group.

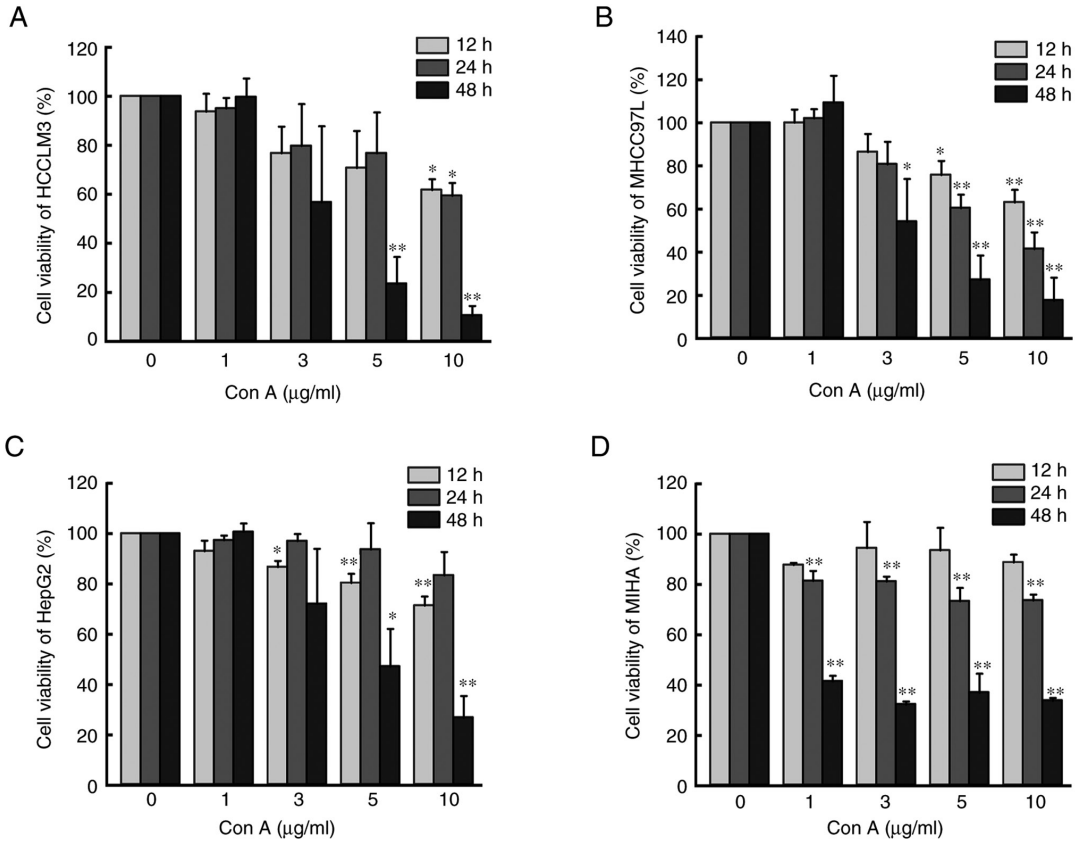

Figure 1. Effect of Con A on the viability of human liver cancer cells and hepatocytes. Cell viability of (A) HCCLM3, (B) MHCC97L, (C) HepG2 and (D) MIHA cells after treatment with Con A (0, 1, 3, 5 and 10 μg/ml) for 12, 24 or 48 h. The data were expressed as the mean ± SD (n=3). *P<0.05 and **P<0.01 vs. the control group. Con A, concanavalin A.

Con A inhibits HCCLM3 cell migration via upregulation of the phosphorylation of ERK1/2, JNK1/2/3 and p38. As demonstrated in Fig. 4, Con A (10 μg/ml) could significantly upregulate the phosphorylation level of ERK1/2, JNK1/2/3 and p38 (P<0.05). To further identify the association between the activation of the MAPK signaling pathway and Con A-mediated inhibition of HCCLM3 cell migration, the ERK1/2 inhibitor U0126, the JNK1/2/3 inhibitor SP600125 and the p38 inhibitor SB203580 were used to detect the roles of the ERK1/2, JNK1/2/3 and p38 signaling, respectively. As revealed in Fig. 5, when the concentration of U0126, SP600125 or SB203580 reached 5 μM, the phosphorylation level of ERK1/2, JNK1/2/3 or p38 they could be restored to that of the control group. Furthermore, inhibition of ERK1/2, JNK1/2/3 or/and p38 signaling also suppressed the Con A-mediated reduction in cell migration, and the cell migration rate recovered from 15% to ~50% (Fig. 6A and B). However, it was found that inhibition of ERK1/2, JNK1/2/3 or/and p38 signaling had no effect on the Con A-mediated inhibition of HCCLM3 cell viability (Fig. 6C).

Con A regulates F-actin redistribution and assembly via ERK1/2, JNK1/2/3 and p38 signaling. Immunofluorescence staining was used to detect F-actin. F-actin was stained red with FITC phalloidin, while the cell nucleus was stained blue with DAPI. As shown in Fig. 7A and B, when analyzing the fluorescence intensity of single cells, it was found that the content of F-actin of individual cells decreased significantly (P<0.05) under the influence of Con A, while inhibition of ERK1/2, JNK1/2/3 or/and p38 signaling could partly recover the content of F-actin decreased by Con A. The spreading area of individual cells was also analyzed. As revealed in Fig. 7A and C, under the influence of Con A, HCCLM3 cells contracted and changed from fibrous to round shape. In addition, inhibition of ERK1/2, JNK1/2/3 or/and p38 signaling could also partly reverse the changes in contraction caused by Con A.

Con A has no effect on the activation of MMP-2 or MMP-9 in HCCLM3 cells. The effect of Con A on the activation of MMP-2 and MMP-9 in HCCLM3 cells was detected by gelatin zymography. In the control group, activated gelatinase MMP-2 and MMP-9 in HCCLM3 cells could degrade gelatin in a polyacrylamide gel, which manifested as white bands. However, after the addition of Con A (10 μg/ml), the optical density of the white bands did not change significantly compared with that of the control group (Fig. 7D-F).

Discussion

In previous studies, Con A was mainly used to establish mouse liver injury models for hepatitis-related research (15,16). By contrast, the present study mainly focused on the anticancer function of Con A and its molecular mechanisms. In the cell viability assay, Con A had a strong inhibitory effect on the viability of human liver cancer cells and normal

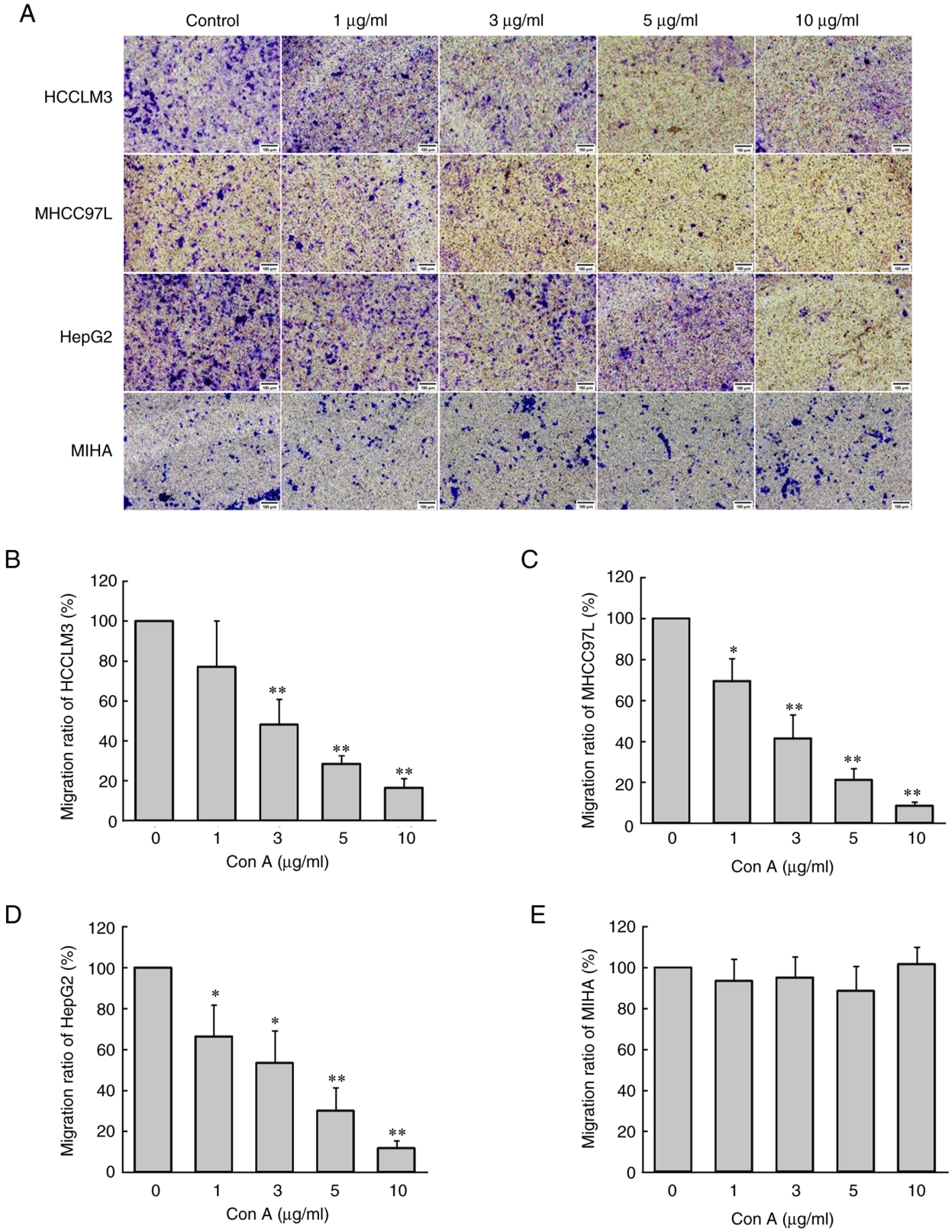

Figure 2. Effect of Con A on the migration of human liver cancer cells and hepatocytes. (A) Cell migration of HCCLM3, MHCC97L, HepG2 and MIHA cells after treatment with Con A (0, 1, 3, 5 and 10 μg/ml) for 6 h. Microscopic imaging of four cell types in a Transwell chamber (scale bar, 100 nm). The quantification of (B) HCCLM3, (C) MHCC97L, (D) HepG2 and (E) MIHA cells in the Transwell chamber was calculated manually by counting the number of cells. The data were expressed as the mean ± SD (n=3). *P<0.05 and **P<0.01 vs. the control group. Con A, concanavalin A.

hepatocytes, which was consistent with the results of previous studies (12,13). In the cell migration assay, Con A could inhibit the migration of HCCLM3, MHCC97L and HepG2 cells completely within 6 h, but had no significant inhibitory effect on MIHA cells. These results demonstrated that Con A had a specific inhibitory effect on liver cancer cell migration.

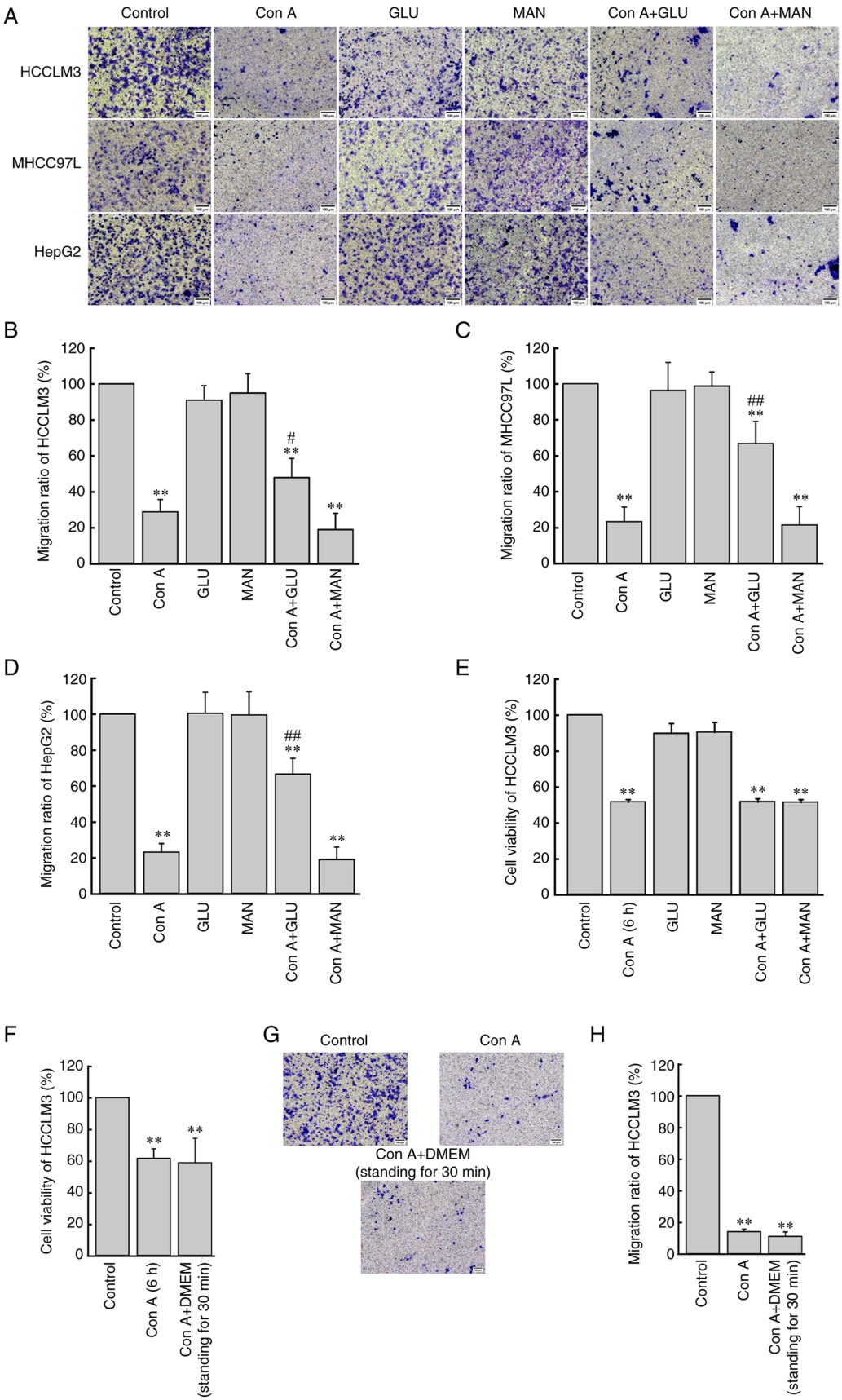

Figure 3. Effect of glucose and mannose-related sugar binding sites on the Con A-mediated regulation of cell migration and viability. (A) Microscopic images of three liver cancer cell lines in a Transwell Boyden Chamber (scale bar, 100 nm). The quantification of (B) HCCLM3, (C) MHCC97L and (D) HepG2 cells in a Transwell chamber was calculated manually by counting the number of cells. (E) Viability of HCCLM3 cells treated with Con A after co-incubation with glucose or mannose for 6 h. (F) Viability of HCCLM3 cells treated with Con A after co-incubation with DMEM for 6 h. (G) Microscopic images of HCCLM3 cell migration in a Transwell chamber (scale bar, 100 nm). (H) Migration of HCCLM3 cells treated with Con A after co-incubation with DMEM for 6 h. The data were expressed as the mean ± SD (n=6). **P<0.01 vs. the control group, $^{\#}$P<0.05 and $^{\#\#}$P<0.01 vs. the Con A group. Con A, concanavalin A (10 μg/ml); GLU, glucose; MAN, mannose.

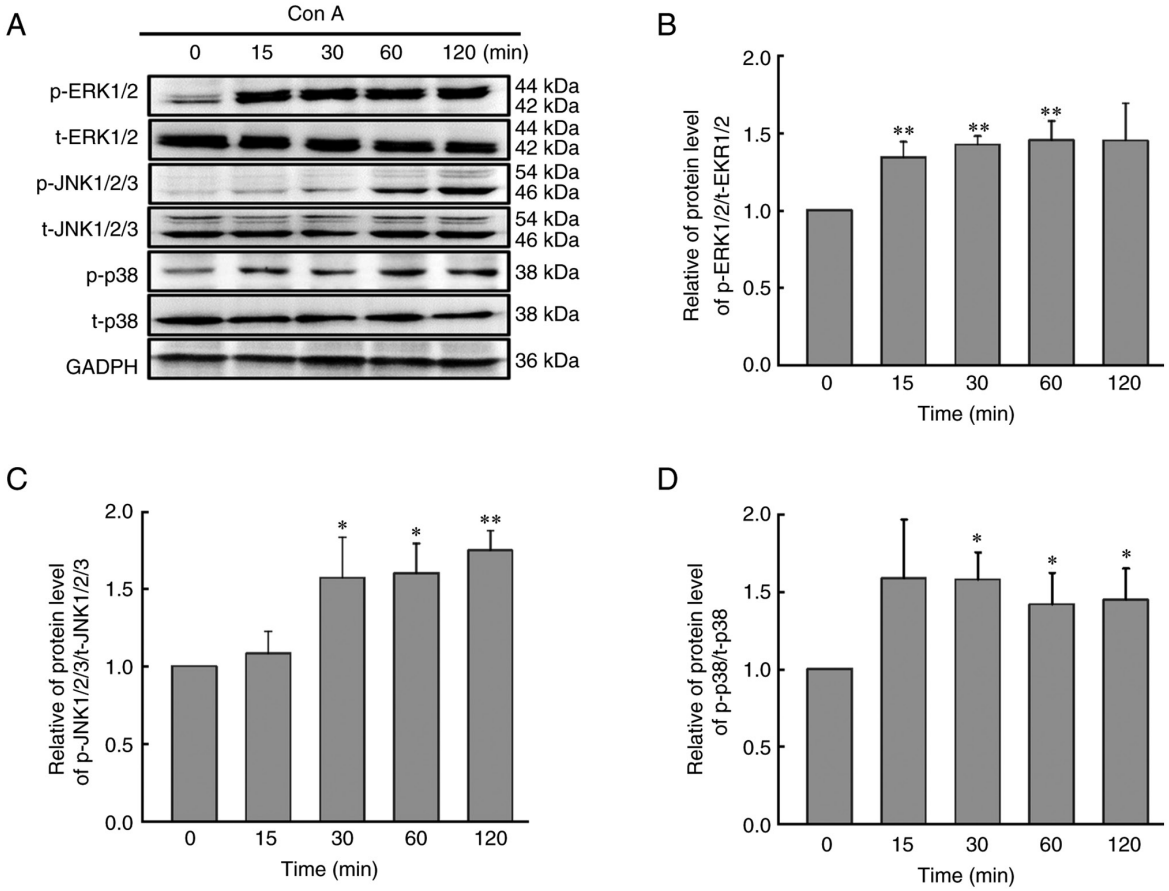

Figure 4. Effect of Con A on the activation of ERK1/2, JNK1/2/3 and p38 in HCCLM3 cells. (A) The expression levels of ERK1/2, JNK1/2/3 and p38 in HCCLM3 cells were analyzed by western blotting. Relative protein level of (B) p-ERK1/2/t-ERK1/2, (C) p-JNK1/2/3/t-JNK1/2/3 and (D) p-p38/t-p38 in HCCLM3 cells. The results of the densitometric analysis of ERK1/2, JNK1/2/3 and p38 activation were normalized to the levels of GAPDH. The data were expressed as the mean ± SD (n=3). *P<0.05 and **P<0.01 vs. the control group. Con A, concanavalin A (10 μg/ml); p, phosphorylated; t, total.

It was hypothesized that, since HepG2 cells have a different tissue origin and degree of malignant metastasis from those of HCCLM3 and MHCC97L cells (17,18), HepG2 cells may have different response patterns to Con A; however, the cell migration assay showed that there was no significant difference in the effects of Con A on HCCLM3, MHCC97L or HepG2 cells. These results suggested that Con A may affect the migration of these cells in a similar way.

To verify whether the effect of Con A on inhibiting the migration of HCCLM3 cells was associated with its effect on inhibiting the viability of HCCLM3 cells, a cell viability assay was conducted within 6 h. The results showed that Con A could reduce the viability of HCCLM3 cells by ~50% within 6 h, while incubation with Con A for a similar time could completely inhibit the migration of HCCLM3 cells. These results indicated that Con A-mediated inhibition of HCCLM3 cell migration was not completely caused by a decline in HCCLM3 cell viability.

Glucose and mannose are isomers, and they both can bind Con A (11). The present study found that Con A inhibits the migration of liver cancer cells only through glucose-related sugar sites. In addition, the effect of glucose or mannose on Con A-mediated inhibition of HCCLM3 cell viability was verified. The results showed that prior co-incubation of glucose or mannose with Con A could not affect the Con A-mediated inhibition of HCCLM3 cell viability, suggesting that Con A did not inhibit the viability of liver cancer cells through glucose or mannose-related pathways. Con A may inhibit liver cancer cell viability via other unknown glycoprotein-related or unrelated molecular pathways. The molecular mechanism of its toxicity needs to be further investigated.

Tumor cells are generally involved in aerobic glycolysis, which leads to a higher demand for glucose in the tumor environment (19,20). When tumor cells were cultured in high-glucose DMEM, in addition to sufficient glucose for biosynthesis, excessive glucose may affect the effect of Con A on tumor cells due to the high affinity of Con A for glucose. Therefore, Con A was co-cultured with DMEM to verify the effect of glucose in DMEM on the viability and migration behavior of HCCLM3 cells. The results showed that co-incubation of Con A with DMEM did not affect the inhibitory effect of Con A on HCCLM3 cell viability or migration. It could be hypothesized that the concentration of glucose in the culture medium may be markedly lower than the glucose-binding quantity of Con A, or the optical activity or/and structure of exogenous glucose may be different from that of the glucose in the culture medium.

The MAPK signaling pathway is one of the most widely studied pathway, and numerous biological behaviors of tumor cells have been associated with the MAPK signaling pathway and its downstream effectors (21-23). Liu *et al* (24) demonstrated that Polygonatum cyrtonema lectin induces

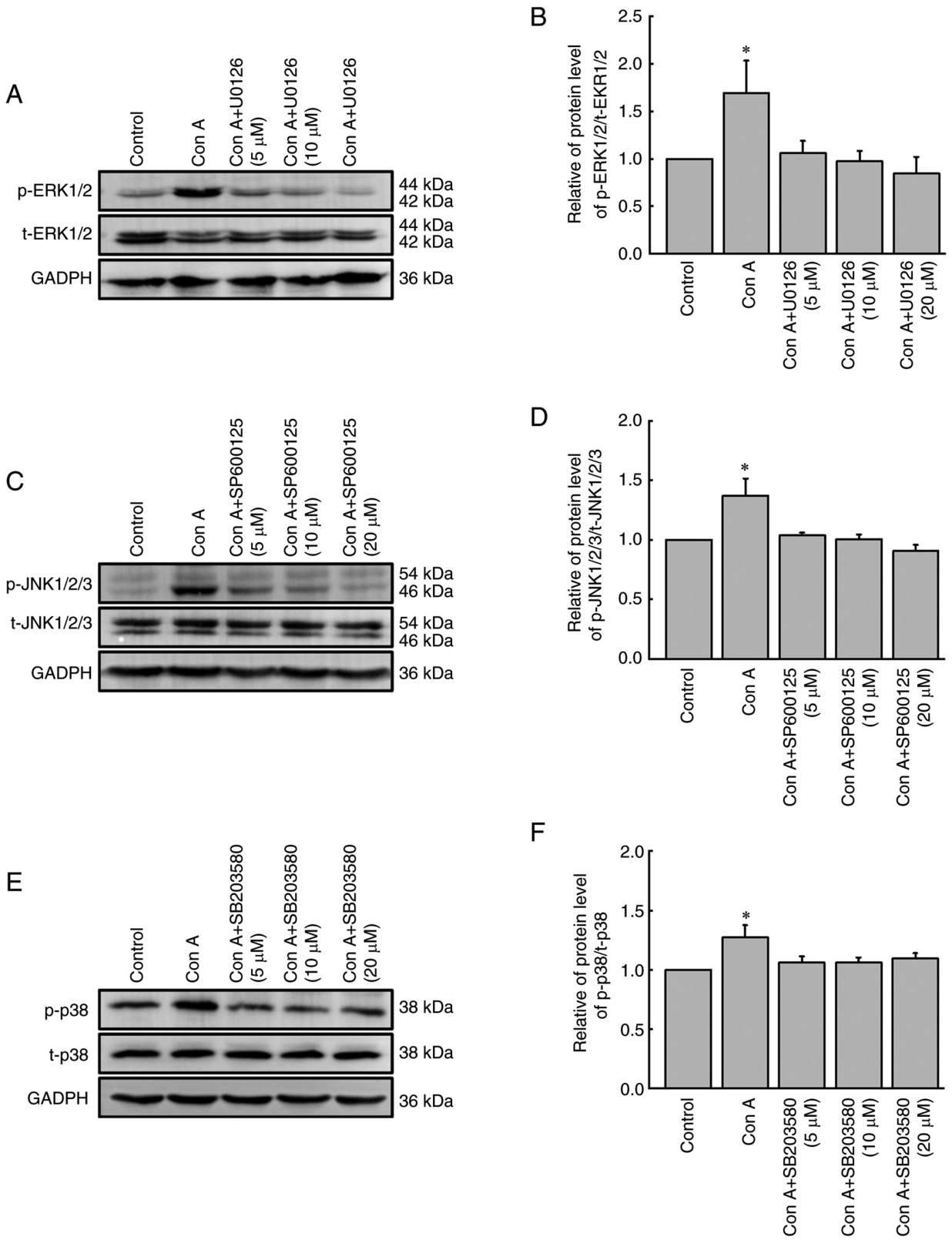

Figure 5. Effect of inhibitors of ERK1/2, JNK1/2/3 and p38 on the activation of ERK1/2, JNK1/2/3 and p38 in HCCLM3 cells. HCCLM3 cells were pre-treated with the ERK1/2 inhibitor U0126, the JNK1/2/3 inhibitor SP600125 or the p38 inhibitor SB203580 for 60 min, and then the expression levels of (A) ERK1/2, (C) JNK1/2/3 and (E) p38 in HCCLM3 cells were analyzed by western blotting. Relative protein level of (B) p-ERK1/2/t-ERK1/2, (D) p-JNK1/2/3/t-JNK1/2/3 and (F) p-p38/t-p38 in HCCLM3 cells. The results of the densitometric analysis of ERK1/2, JNK1/2/3 and p38 activation were normalized to the levels of GAPDH. The data were expressed as the mean ± SD (n=3). *P<0.05 vs. the control group. Con A, concanavalin A (10 μg/ml); p, phosphorylated; t, total.

the apoptosis and autophagy of human lung adenocarcinoma A549 cells through the MAPK signaling pathway. The current study found that Con A could upregulate the phosphorylation levels of ERK1/2, JNK1/2/3 and p38 within 2 h. Moreover, inhibition of ERK1/2, JNK1/2/3 or/and p38 signaling also suppressed the Con A-mediated reduction in

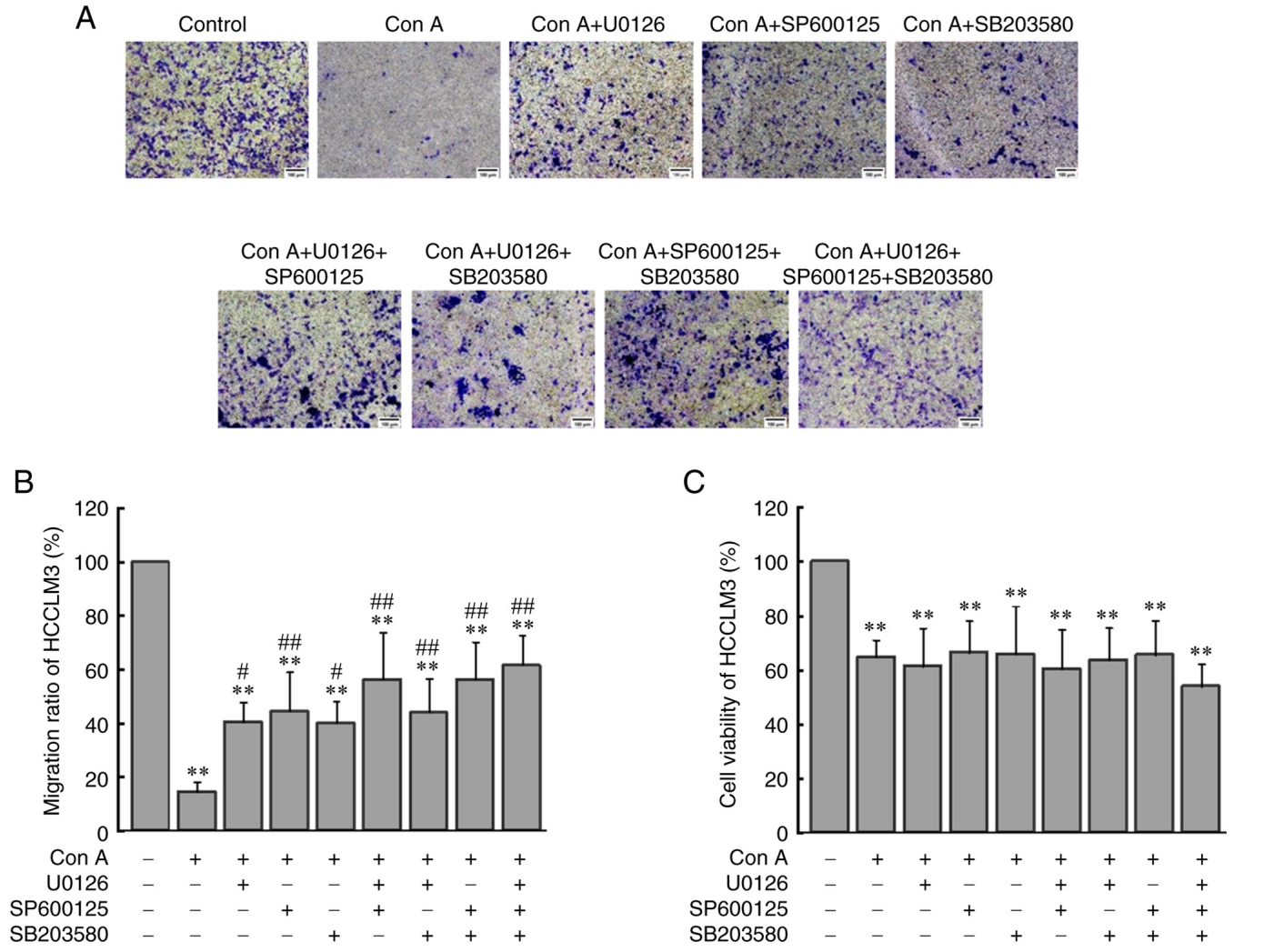

Figure 6. Effect of inhibitors of ERK1/2, JNK1/2/3 and p38 on the migration and viability of HCCLM3 cells. HCCLM3 cells were pre-treated with the ERK1/2 inhibitor U0126, the JNK1/2/3 inhibitor SP600125 or/and the p38 inhibitor SB203580 for 60 min, and then cell migration and viability upon Con A treatment were detected. (A) Microscopic images of HCCLM3 cells in a Transwell chamber (scale bar, 100 nm). (B) The quantification of HCCLM3 cells in a Transwell chamber was performed by counting the number of cells. **P<0.01 vs. the control group; $^{\#}$P<0.05 and $^{\#\#}$P<0.01 vs. the Con A group. (C) HCCLM3 cell viability. **P<0.01 vs. the control group. The data were expressed as the mean ± SD (n=6). Con A, concanavalin A (10 μg/ml).

cell migration. These results indicated that Con A inhibited HCCLM3 cell migration through the ERK1/2, JNK1/2/3 and p38 signaling pathways. In addition, it was found that the addition of inhibitors of the aforementioned three signaling pathways did not affect the Con A-mediated inhibition of HCCLM3 cell viability. Combined with the results of the sugar inhibition assay, it was concluded that the molecular mechanism of Con A-mediated altered HCCLM3 cell viability was different from that of Con A-mediated altered HCCLM3 cell migration.

In tumor cells, the depolymerization and polymerization of F-actin play important roles in cell migration and invasion (25,26). In addition, changes in cell morphology or contractility can also affect tumor cell metastasis (27). In the present study, when HCCLM3 cells were exposed to Con A for 6 h, the spreading area of individual cells decreased significantly, and the cells changed shape from long spindle to round. Upon analyzing and quantifying the fluorescence intensity of individual cells, the content of F-actin in HCCLM3 cells was observed to decrease significantly compared with that of the control group. Although the fluorescence intensity of F-actin in the Con A group appeared visually to be stronger than that of the control group, considering that the cell spreading area of HCCLM3 cells in the Con A group was also reduced, the relative fluorescence intensity of F-actin of single cells in the Con A group was lower than that of the control group. Moreover, inhibition of ERK1/2, JNK1/2/3 or/and p38 signaling could partly restore the Con A-mediated reduction in cell spreading area and F-actin content. These results showed that Con A could regulate F-actin redistribution and assembly via the MAPK signaling pathway. Previous studies also showed that the MAPK signaling pathway could affect the polymerization of F-actin, thus affecting the metastasis of tumor cells (28,29).

The migration ability of tumor cells is usually associated with the activities of the gelatinases MMP-2 and MMP-9 (30,31). Jian *et al* (32) found that Bandeiraea simplicifolia lectin could bind to N-acetylgalactosamine in hepatoma cells, thus affecting the expression of MMP-2 and MMP-9 to inhibit cell migration. However, the present study found that Con A had no significant effect on the activities of MMP-2 or

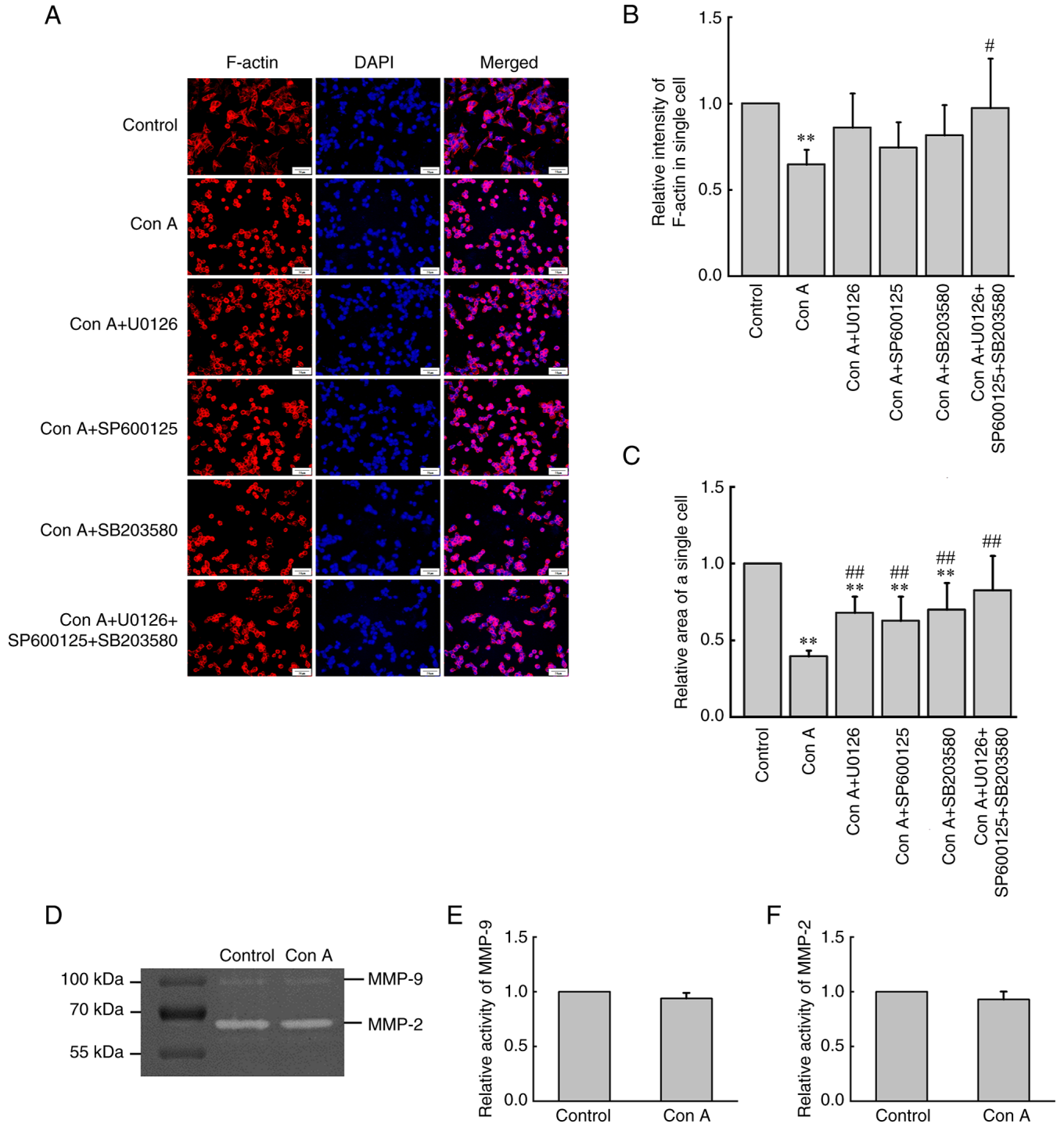

Figure 7. Effect of Con A on F-actin and MMPs in HCCLM3 cells. (A) Fluorescence microscopic images of F-actin and cell nucleus (scale bar, 50 nm); (B) F-actin fluorescence intensity of individual cells in each group (n=40). **P<0.01 vs. the control group; $^{\#}$P<0.05 vs. the Con A group. (C) Analysis of spreading area of single HCCLM3 cells (n=40). **P<0.01 vs. the control group; $^{\#\#}$P<0.01 vs. the Con A group. (D) MMP-2 and MMP-9 under white light transmission in cells treated with Con A. Activation of (E) MMP-9 and (F) MMP-2 upon optical density analysis (n=3). The data were expressed as the mean ± SD. Con A, concanavalin A (10 μg/ml); F-actin, fibrous-actin. MMP, matrix metalloproteinase.

MMP-9 in HCCLM3 cells, indicating that there were significant differences in the response mechanism of different plant lectins.

In summary, the present study reported the effect of Con A on the viability and migration of human liver cancer cells and hepatocytes, and preliminary discussed the molecular mechanism of Con A affecting HCCLM3 cell migration. Studying the association between the specific sugar-binding ability of different plant lectins and the glycosylation variation of different tumor cells can increase the understanding of tumor cells and their glycosylation changes, as well as provide a new insight for plant lectins as potential anticancer agents.

Acknowledgements

Not applicable.

Funding

The present study was supported by the Science and Technology Research Program of Chongqing Municipal Education Commission (grant no. KJQN201800601) and the Natural Science Foundation of Chongqing (grant no. cstc2020jcyj-msxmX0760).

Availability of data and materials

The datasets used and/or analyzed during the current study are available from the corresponding author on reasonable request.

Authors' contributions

BZ and HJ designed the study. HJ, XW and XZ performed the experiments. HJ analyzed the data and drafted the initial manuscript. BZ supervised the present study and revised the manuscript. BZ and HJ confirm the authenticity of all the raw data. All authors have read and approved the final manuscript.

Ethics approval and consent to participate

Not applicable.

Patient consent for publication

Not applicable.

Competing interests

The authors declare that they have no competing interests.

References

1. Yuan H, Ji J, Shi M, Shi Y, Liu J, Wu J, Yang C, Xi W, Li Q, Zhu W, *et al*: Characteristics of pan-cancer patients with ultra-high tumor mutation burden. Front Oncol 11: 682017, 2021.
2. Li Y, Zhou Y, Mao F, Shen S, Zhao B, Xu Y, Lin Y, Zhang X, Cao X, Xu Y, *et al*: mir-452 reverses abnormal glycosylation modification of ERα and estrogen resistance in TNBC (triple-negative breast cancer) through targeting UGT1A1. Front Oncol 10: 1509, 2020.
3. Fan C, Tu C, Qi P, Guo C, Xiang B, Zhou M, Li X, Wu X, Li X, Li G, *et al*: GPC6 promotes cell proliferation, migration, and invasion in nasopharyngeal carcinoma. J Cancer 10: 3926-3932, 2019.
4. Kannagi R: Carbohydrate antigen sialyl Lewis 1- its pathophysiological significance an induction mechanism in cancer progression. Chang Gung Med J 30: 189-209, 2007.
5. Miyagi T, Takahashi K, Hata K, Shiozaki K and Yamaguchi K: Sialidase significance for cancer progression. Glycoconj J 29: 567-577, 2012.
6. Estrada-Martínez LE, Moreno-Celis U, Cervantes-Jiménez R, Ferriz-Martínez RA, Blanco-Labra A and García-Gasca T: Plant lectins as medical tools against digestive system cancers. Int J Mol Sci 18: 1403, 2017.
7. Oliveira I, Nunes A, Lima A, Borralho P, Rodrigues C, Ferreira RB and Ribeiro AC: New lectins from mediterranean flora. Activity against ht29 colon cancer cells. Int J Mol Sci 20: 3059, 2019.
8. Lawanprasert A, Guinan CA, Langford EA, Hawkins CE, Sloand JN, Fescemyer HW, Aronson MR, Halle JA, Marden JH and Medina SH: Discovery of antitumor lectins from rainforest tree root transcriptomes. PLoS One 15: e0229467, 2020.
9. Bloise N, Okkeh M, Restivo E, Della PC and Visai L: Targeting the 'sweet side' of tumor with glycan-binding molecules conjugated-nanoparticles: Implications in cancer therapy and diagnosis. Nanomaterials 11: 289, 2021.
10. He Z, Chen Q, Chen F, Zhang J, Li H and Lin JM: DNA-mediated cell surface engineering for multiplexed glycan profiling using MALDI-TOF mass spectrometry. Chem Sci 7: 5448-5452, 2016.
11. Cavada BS, Pinto-Junior VR, Osterne VJ and Nascimento KS: ConA-like lectins: High similarity proteins as models to study structure/biological activities relationships. Int J Mol Sci 20: 30, 2018.
12. Lei HY and Chang CP: Lectin of Concanavalin A as an anti-hepatoma therapeutic agent. J Biomed Sci 16: 10, 2009.
13. Lai YC, Chuang YC, Chang CP and Yeh TM: Macrophage migration inhibitory factor has a permissive role in concanavalin A-induced cell death of human hepatoma cells through autophagy. Cell Death Dis 6: e2008, 2015.
14. Chang CP, Yang MC, Liu HS, Lin YS and Lei HY: Concanavalin A induces autophagy in hepatoma cells and has a therapeutic effect in a murine in situ hepatoma model. Hepatology 45: 286-296, 2007.
15. Lai AC, Chi PY, Thio CL, Han YC, Kao HN, Hsieh HW, Gervay-Hague J and Chang YJ: α-lactosylceramide protects against iNKT-mediated murine airway hyperreactivity and liver injury through competitive inhibition of Cd1d binding. Front Chem 7: 811, 2019.
16. Li S, Bi Y, Wang Q, Xu M, Ma Z, Yang Y, Chang Y, Chen S, Liu D, Duan Z, *et al*: Transplanted mouse liver stem cells at different stages of differentiation ameliorate concanavalin A-induced acute liver injury by modulating tregs and Th17 cells in mice. Am J Trans Res 11: 7324-7337, 2019.
17. Luo G, Chao YL, Tang B, Li BS, Xiao YF, Xie R, Wang SM, Wu YY, Dong H, Liu XD and Yang SM: miR-149 represses metastasis of hepatocellular carcinoma by targeting actin-regulatory proteins PPM1F. Oncotarget 6: 37808-37823, 2015.
18. Zhang Y, Hu MY, Wu WZ, Wang ZJ, Zhou K, Zha XL and Liu KD: The membrane-cytoskeleton organizer ezrin is necessary for hepatocellular carcinoma cell growth and invasiveness. J Cancer Res Clin Oncol 132: 685-697, 2006.
19. Yang LN, Ning ZY, Wang L, Yan X and Meng ZQ: HSF2 regulates aerobic glycolysis by suppression of FBP1 in hepatocellular carcinoma. Am J Cancer Res 9: 1607-1621, 2019.
20. Liu Y, Zhang Y, Xiao B, Tang N, Hu J, Liang S, Pang Y, Xu H, Ao J, Yang J, *et al*: MiR-103a promotes tumour growth and influences glucose metabolism in hepatocellular carcinoma. Cell Death Dis 12: 618, 2021.
21. Du P, Liang H, Fu X, Wu P, Wang C, Chen H, Zheng B, Zhang J, Hu S, Zeng R, *et al*: SLC25A22 promotes proliferation and metastasis by activating MAPK/ERK pathway in gallbladder cancer. Cancer Cell Int 19: 33, 2019.
22. Chen J, Ji T, Wu D, Jiang S, Zhao J, Lin H and Cai X: Human mesenchymal stem cells promote tumor growth via MAPK pathway and metastasis by epithelial mesenchymal transition and integrin α5 in hepatocellular carcinoma. Cell Death Dis 10: 425, 2019.
23. Zhang YP, Liu KL, Yang Z, Lu BS, Qi JC, Han ZW, Yin YW, Zhang M, Chen DM, Wang XW, *et al*: The involvement of FBP1 in prostate cancer cell epithelial mesenchymal transition, invasion and metastasis by regulating the MAPK signaling pathway. Cell Cycle 18: 2432-2446, 2019.
24. Liu T, Wu L, Wang D, Wang H, Chen J, Yang C, Bao J and Wu C: Role of reactive oxygen species-mediated MAPK and NF-κB activation in polygonatum cyrtonema lectin-induced apoptosis and autophagy in human lung adenocarcinoma A549 cells. J Biochem 160: 315-324, 2016.
25. Zhang X, Xu L and Yang T: miR-31 modulates liver cancer HepG2 cell apoptosis and invasion via ROCK1/F-actin pathways. OncoTargets Ther 13: 877-888, 2020.
26. Schneiderman RS, Giladi M, Zeevi E, Voloshin T, Shteingauz A, Porat Y, Munster M, Kirson E, Weinberg U and Palti Y: Angi-11. tumor treating fields (ttfields) inhibit cancer cell migration and invasion by inducing reorganization of the actin cytoskeleton and formation of cell adhesions. Neuro Oncol 20 (Suppl 6): vi30, 2018.
27. Gkretsi V and Stylianopoulos T: Cell adhesion and matrix stiffness: Coordinating cancer cell invasion and metastasis. Front Oncol 8: 145, 2018.
28. Rudzka DA, Mason S, Neilson M, McGarry L, Kalna G, Hedley A, Blyth K and Olson MF: Selection of established tumour cells through narrow diameter micropores enriches for elevated Ras/Raf/MEK/ERK MAPK signalling and enhanced tumour growth. Small GTPases 12: 294-310, 2020.

29. Ni Y, Wang X, Yin X, Li Y, Liu X, Wang H, Liu X, Zhang J, Gao H, Shi B and Zhao S: Plectin protects podocytes from adriamycin-induced apoptosis and F-actin cytoskeletal disruption through the integrin α6β4/FAK/p38 MAPK pathway. J Cell Mol Med 22: 5450-5467, 2018.
30. Kwon Y, Park SJ, Nguyen BT, Kim MJ, Oh S, Lee H, Park N, Kim HS, Kang MJ, Min BS, *et al*: Multi-layered proteogenomic analysis unravels cancer metastasis directed by MMP-2 and focal adhesion kinase signaling. Sci Rep 11: 17130, 2021.
31. Lu J, Wang Z, Li S, Xin Q, Yuan M, Li H, Song X, Gao H, Pervaiz N, Sun X, *et al*: Quercetin inhibits the migration and invasion of HCCLM3 cells by suppressing the expression of p-Akt1, matrix metalloproteinase (MMP) MMP-2, and MMP-9. Med Sci Monit 24: 2583-2589, 2018.
32. Jian Q, Yang Z, Shu J, Liu XW, Zhang J and Zheng L: Lectin BS-I inhibits cell migration and invasion via AKT/GSK-3β/β-catenin pathway in hepatocellular carcinoma. J Cell Mol Med 22: 315-329, 2018.